A Gaussian Plume Model of Atmospheric Dispersion Based on Second-Order Closure

R. I. SYKES, W. S. LEWELLEN AND S. F. PARKER

Aeronautical Research Associates of Princeton, Inc., Princeton, NJ 08540

(Manuscript received 23 February 1985, in final form 18 September 1985)

ABSTRACT

A practical model of atmospheric dispersion of a passive tracer based on systematic reduction of the second-order closure transport equations using Gaussian shape assumptions is presented. The model is comparable with conventional Gaussian plume models in complexity, but still maintains the capability to also predict concentration fluctuation variance and to utilize direct measurements of turbulent velocity variances in a consistent manner. Comparison with laboratory data demonstrates the model's ability to produce reasonable predictions for the concentration field.

1. Introduction

In a recent paper, Sykes et al. (1984; referred to as SLP hereafter) presented a system of transport equations for the second-order correlations of passive scalar fluxes and fluctuations, and demonstrated their ability to predict dispersion characteristics in a wind-tunnel boundary layer. Although these equations are a complicated set of nonlinear, coupled partial differential equations, SLP noted that the flux-transport model does provide a very general framework within which complex flow effects can be considered. This framework also provides the opportunity for systematic simplification of the equations to produce reduced models with smaller computational requirements. In this paper, we still consider a passive source of pollutant, but we present a reduction of the transport equations to the level of a conventional Gaussian plume model, requiring only the solution of a small number of ordinary differential equations.

Since the model represents the pollutant field as a steady plume, it will suffer the same types of restriction as the usual Gaussian plume models, e.g., variable wind cases cannot be accurately dealt with. However, we believe the model has two advantages over conventional Gaussian plume models. First and probably most important, by providing a model for the concentration variance as well as the mean, we provide the possibility of systematic estimates of the expected predictability of individual concentration samples as outlined by Lewellen and Sykes (1983). Second, using turbulent flow data as a direct input into the model, we decouple the specification of the diffusing environment from the dispersion model. If measurements are available, they can be used to define the atmospheric state; if not, then a model atmosphere must be specified using whatever data is available. By treating the specification of the diffusing environment separately from the solution of the dispersion model we maintain the ability to improve both parts independently. Other Gaussian plume models have been formulated to utilize direct measurements of wind variances (see Pasquill and Smith, 1983). These previous models have been based on empirical correlations between plume spread and turbulence. We attempt to derive our model by consistent approximations to a much more complex set of transport equations.

In the next section, we derive the plume equations from the full transport equations of SLP. The model predictions are compared with some laboratory flow data in section 3, and some extensions of the simple model are described in section 4.

2. Derivation of the plume equations

The technique that we employ to reduce the transport equations is the standard moment method, which integrates the equations and their various moments in the plane transverse to the plume transport direction. We first derive the equation for homogeneous turbulence to give a clear picture of the model, and later examine several extensions and effects of flow inhomogeneity. The homogeneous equations have been briefly described by Lewellen (1981), and also in SLP, but we now derive them systematically.

The transport equation for mean scalar concentration C is

$$U\frac{\partial C}{\partial x} = -\frac{\partial}{\partial y}\overline{v'c'} - \frac{\partial}{\partial z}\overline{w'c'}, \tag{1}$$

where U is the mean flow speed in the x-direction, a prime denotes a fluctuation from the mean, and the overbar denotes an ensemble average value. Equation (1) is to be solved subject to the initial condition

$$C(0, y, z) = C_0(y, z), \tag{2}$$

which defines the source distribution.

We define angular brackets to represent integration in the cross-stream plane, i.e.,

$$\langle \phi \rangle = \int_{-\infty}^{\infty} \int_{-\infty}^{\infty} \phi dy dz,$$

then we can immediately write the conservation of scalar flux as

$$U \frac{d}{dx} \langle C \rangle = 0, \tag{3}$$

i.e., $\langle C \rangle = \langle C_0 \rangle$. If we define the plume centroid $(\bar{y}, \bar{z})$, in the obvious way, as

$$\bar{y} = \frac{\langle yC \rangle}{\langle C \rangle}, \quad \bar{z} = \frac{\langle zC \rangle}{\langle C \rangle},$$

then multiplying (1) by y, we obtain

$$U \frac{d}{dx} \langle yC \rangle = U \langle C \rangle \frac{d\bar{y}}{dx}$$

$$= \left\langle -y \frac{\partial}{\partial y} \overline{v'c'} \right\rangle + \left\langle -y \frac{\partial}{\partial z} \overline{w'c'} \right\rangle$$

$$= \langle \overline{v'c'} \rangle.$$

Thus,

$$U \frac{d\bar{y}}{dx} = \frac{\langle \overline{v'c'} \rangle}{\langle C \rangle} \tag{4}$$

and similarly

$$U \frac{d\bar{z}}{dx} = \frac{\langle \overline{w'c'} \rangle}{\langle C \rangle}. \tag{5}$$

We extend the moment equations to the diagonal second moments before considering the second-order correlations on the rhs of Eqs. (4) and (5). Define

$$\sigma_y^2 = \frac{\langle y'^2 C \rangle}{\langle C \rangle}, \quad \sigma_z^2 = \frac{\langle z'^2 C \rangle}{\langle C \rangle},$$

where $y' = y - \bar{y}$, $z' = z - \bar{z}$, and multiply (1) by y'^2 to obtain

$$U \frac{d}{dx} \langle y'^2 C \rangle = U \langle C \rangle \frac{d}{dx} \sigma_y^2$$

$$= \left\langle -y'^2 \frac{\partial}{\partial y} \overline{v'c'} \right\rangle - \left\langle y'^2 \frac{\partial}{\partial z} \overline{w'c'} \right\rangle$$

$$= 2 \langle y' \overline{v'c'} \rangle,$$

i.e.,

$$U \frac{d}{dx} \sigma_y^2 = 2 \frac{\langle y' \overline{v'c'} \rangle}{\langle C \rangle}, \tag{6}$$

and similarly

$$U \frac{d}{dx} \sigma_z^2 = 2 \frac{\langle z' \overline{w'c'} \rangle}{\langle C \rangle}. \tag{7}$$

Equations (3)–(7) are the moment equations for the mean concentration, but they contain second-order terms that must be specified before the system is closed. This is the turbulence closure requirement, which we achieve by use of the second-order closure assumptions as described in SLP. We write transport equations for the fluxes $\overline{v'c'}$, $\overline{w'c'}$ as follows:

$$U \frac{\partial}{\partial x} \overline{v'c'} = -\overline{v'^2} \frac{\partial C}{\partial y} + v_c \frac{\partial}{\partial y} \left(q\Lambda \frac{\partial}{\partial y} \overline{v'c'} \right)$$

$$+ v_c \frac{\partial}{\partial z} \left(q\Lambda \frac{\partial}{\partial z} \overline{v'c'} \right) - \frac{Aq}{\Lambda} \overline{v'c'} \tag{8}$$

$$U \frac{\partial}{\partial x} \overline{w'c'} = -\overline{w'^2} \frac{\partial C}{\partial z} + \frac{g}{T_0} \overline{c'\theta'} + v_c \frac{\partial}{\partial y} \left(q\Lambda \frac{\partial}{\partial y} \overline{w'c'} \right)$$

$$+ v_c \frac{\partial}{\partial z} \left(q\Lambda \frac{\partial}{\partial z} \overline{w'c'} \right) - \frac{Aq}{\Lambda} \overline{w'c'} \tag{9}$$

where v_c, A are empirical closure constants with values 0.3 and 0.75, respectively, g is gravitational acceleration, T_0 is the mean temperature, and θ' is the temperature fluctuation. The modeled terms that contain the original constants represent the third-order correlation as a gradient diffusion term, and the pressure correlation by the simple return-to-isotropy model; $q^2 = \overline{u'^2} + \overline{v'^2} + \overline{w'^2}$ is twice the turbulent kinetic energy, and Λ is a turbulence length scale. We note that we have also assumed the Reynolds stress tensor to be diagonal in this homogeneous flow, since there are no velocity gradients. The same closure is used for either stable or unstable flow. The difference is expected to come in through the different character of the turbulence.

We can now close the moment equations by taking the appropriate moments of (8) and (9), e.g.

$$U \frac{d}{dx} \langle \overline{v'c'} \rangle = -\overline{v'^2} \left\langle \frac{\partial C}{\partial y} \right\rangle$$

$$+ \left\langle v_c \frac{\partial}{\partial y} \left(q\Lambda \frac{\partial}{\partial y} \overline{v'c'} \right) \right\rangle - \frac{Aq}{\Lambda} \langle \overline{v'c'} \rangle,$$

which reduces, after integration to

$$U \frac{d}{dx} \langle \overline{v'c'} \rangle = -\frac{Aq}{\Lambda} \langle \overline{v'c'} \rangle. \tag{10}$$

Similarly

$$U \frac{d}{dx} \langle \overline{w'c'} \rangle = \frac{g}{T_0} \langle \overline{c'\theta'} \rangle - \frac{Aq}{\Lambda} \langle \overline{w'c'} \rangle. \tag{11}$$

Also

$$U \frac{d}{dx} \langle y' \overline{v'c'} \rangle = \overline{v'^2} \langle C \rangle - \frac{Aq}{\Lambda} \langle y' \overline{v'c'} \rangle, \tag{12}$$

$$U \frac{d}{dx} \langle z' \overline{w'c'} \rangle = \overline{w'^2} \langle C \rangle + \frac{g}{T_0} \langle z' \overline{c'\theta'} \rangle - \frac{Aq}{\Lambda} \langle z' \overline{w'c'} \rangle. \tag{13}$$

We still require moments of the temperature correlation, $\overline{c'\theta'}$, to close the system, which we obtain from the transport equation:

$$U\frac{\partial}{\partial x}\overline{c'\theta'} = -\overline{w'c'}\frac{dT}{dz} - \overline{w'\theta'}\frac{\partial C}{\partial z} + v_c\frac{\partial}{\partial y}\left(q\Lambda\frac{\partial}{\partial y}\overline{c'\theta'}\right) - 2bs\frac{q}{\Lambda}\overline{c'\theta'},$$

where $s = 1.8$ (Lewellen, 1977), and we have permitted a uniform temperature gradient and heat flux in our homogeneous problem. Moments of this equation give

$$U\frac{d}{dx}\langle\overline{c'\theta'}\rangle = -\frac{dT}{dz}\langle\overline{w'c'}\rangle - 2bs\frac{q}{\Lambda}\langle\overline{c'\theta'}\rangle \quad (14)$$

$$U\frac{d}{dx}\langle z'\overline{c'\theta'}\rangle = -\frac{dT}{dz}\langle z'\overline{w'c'}\rangle + \overline{w'\theta'}\langle C\rangle - 2bs\frac{q}{\Lambda}\langle z'\overline{c'\theta'}\rangle. \quad (15)$$

Equations (10)–(15) complete the system of equations for the mean concentration, apart from initial conditions on the second-order correlation moments, which we assume are all zero, i.e., there is no initial correlation between concentration fluctuations and the flow field. Using these initial conditions, it is easy to see that the homogeneity of (4), (5), (10), (11), and (14) imply $\bar{y} = \bar{y}_0$, $\bar{z} = \bar{z}_0$, and $\langle\overline{v'c'}\rangle = \langle\overline{w'c'}\rangle = \langle\overline{c'\theta'}\rangle = 0$, where $\bar{y}_0$, $\bar{z}_0$ is the centroid of the source distribution. Thus, in the homogeneous case, we have a reduced set of equations to solve, namely (6), (7), (12), (13), and (15). For constant turbulence conditions, these equations are easy to solve analytically, and give

$$\sigma_y^2 - \sigma_{y0}^2 = \frac{2\Lambda^2\overline{v^2}}{A^2q^2}\left(\frac{Aqx}{\Lambda U} - 1 + e^{-Aqx/\Lambda U}\right), \quad (16)$$

which agrees with Taylor's (1921) theory for an exponential autocorrelation, and an integral time scale of Λ/Aq.

The vertical spread is more complicated, being influenced by buoyancy fluctuations, but can be written as

$$\sigma_z^2 - \sigma_{z0}^2 = 2\left[\frac{Kx}{U} + A_+(1 - e^{r_+x/U}) + A_-(1 - e^{r_-x/U})\right], \quad (17)$$

where

$$K = \frac{g\overline{w'\theta'}/T_0 + 2bsq\overline{w^2}/\Lambda}{N^2 + 2Absq^2/\Lambda^2}$$

$$r_\pm = -\frac{2bs + Aq/\Lambda \pm [(2bs - A)^2q^2/\Lambda^2 - 4N^2]^{1/2}}{2}$$

$$A_\pm = \mp\frac{Kr_\mp + \overline{w^2}}{r \pm (r_+ - r_-)}$$

$$N^2 = \frac{g}{T_0}\frac{dT}{dz}$$

The result (17) is seen to collapse to (16) if $\overline{w'\theta'} = N^2 = 0$, and also shows that the late-time effective diffusivity, K, does depend on buoyancy effects in the expected way, i.e., K is reduced when $\overline{w'\theta'} < 0$ and $N^2 > 0$. The general dependence of σ_z on $qx/\Lambda U$ is roughly similar throughout the stability range, but there are two separate decay rates toward the late-time effective diffusivity. Equation (17) illustrates the model dependence on atmospheric stability in a manner that does not require any empirical classification scheme.

In addition to moments of the mean concentration, SLP shows how to construct an equation for the integral of the scalar fluctuation variance, $\overline{c'^2}$. We simply reproduce those equations here, without derivation.

$$U\frac{d}{dx}\langle\overline{c'^2}\rangle = -U\frac{d}{dx}\langle C^2\rangle - \alpha_c\frac{q_c}{\Lambda_c}\langle\overline{c'^2}\rangle. \quad (18)$$

We approximate $\langle C^2\rangle$ using the assumption of Gaussian shape to obtain

$$\langle C^2\rangle = \frac{\langle C\rangle^2}{4\pi\sigma_y\sigma_z}.$$

The values q_c and Λ_c are velocity and length scales for the scalar fluctuations, and are specified in SLP as follows:

For $\Lambda_c < 0.41\Lambda$:

$$q_c = q\left(\frac{\Lambda_c}{\Lambda}\right)^{1/3}, \quad \frac{d\Lambda_c}{dt} = 0.54q_c, \quad \alpha_c = 0.34 \quad (19a)$$

For $\Lambda_c > 0.41\Lambda$:

$$q_c = q, \quad \frac{d\Lambda_c}{dt} = 0.1q\frac{\Lambda}{\Lambda_c}, \quad \alpha_c = 0.4 \quad (19b)$$

The initial condition for the fluctuation scale is $\Lambda_c = \sigma_0$, which is the source size, and the numerical constants in (19) are derived in SLP by matching the results of the model equation with the data of Fackrell and Robins (1982). Essentially, (19a) gives the inertial-range scaling laws for small plumes and thus correctly predicts source-size dependence, while (19b) describes the late-time behavior of the fluctuation timescale. The latter is much less certain than the early time results, and our simple model may therefore require modification as our understanding improves.

At this point, we have a relatively small set of ordinary differential equations which will predict the mean and fluctuation variance in a plume in homogeneous turbulence. In the next section, we show several examples of results from the simple model.

3. A simple, practical plume model

If a model is to be used for practical prediction purposes, then it must be able to deal with realistic atmospheric profiles of mean and turbulent quantities, i.e., we must relax the requirement of homogeneity. The simplest way to do this is to leave the model equations unchanged, but interpret the flow variables to mean the local values at the location of the plume. We can account for the spread of the plume by defining the local value as an average over the region occupied by the mean concentration field. Our plume equations can therefore be written as

$$U\frac{d}{dx}\langle C\rangle = 0 \tag{20a}$$

$$U\frac{d}{dx}\sigma_y^2 = 2F_y \tag{20b}$$

$$U\frac{d}{dx}\sigma_z^2 = 2F_z \tag{20c}$$

$$U\frac{d}{dx}F_y = \overline{v'^2} - A\frac{q}{\Lambda_H}F_y \tag{20d}$$

$$U\frac{d}{dx}F_z = \overline{w'^2} + \frac{g}{T_0}G - A\frac{q_s}{\Lambda}F_z \tag{20e}$$

$$U\frac{d}{dx}G = -F_z\frac{dT}{dz} + \overline{w'\theta'} - \frac{2bsq_s}{\Lambda}G, \tag{20f}$$

where we have defined

$$F_y = \frac{\langle y'\overline{v'c'}\rangle}{\langle C\rangle}, \quad F_z = \frac{\langle z'\overline{w'c'}\rangle}{\langle C\rangle}, \quad G = \frac{\langle z'\overline{c'\theta'}\rangle}{\langle C\rangle},$$

$$\bar{y} = y_0, \quad \bar{z} = z_0.$$

All background flow variables in (20) refer to an average value over the plume, and for definiteness we shall use a triangular weighted average over the range $\bar{z} \pm 2\sigma_z$. We have also included the possibility of different horizontal and vertical scales represented by the variables q_s and Λ_H. This is in recognition of the fact that in convective boundary layers, there are large-scale eddies that extend to the surface where they are purely horizontal. This gives long time scales for horizontal motions near the boundary, while the vertical motions are restricted by the presence of the solid surface and are consequently much smaller and faster. Thus, q_s^2 represents the energy in the small eddies with scale Λ, while q^2 is the total energy and Λ_H is a horizontal scale. Evidence of the difference in scales for the vertical and horizontal motions is given by Kaimal (1978), who shows a constant length scale for the horizontal fluctuations as the surface is approached, while the scale for $\overline{w'^2}$ tends linearly to zero. Specification of the two scales will be discussed further when we present results for some dispersion experiments.

Since the horizontal motions will be dominant in producing concentration fluctuations via plume meandering, the fluctuation variance equation becomes

$$U\frac{d}{dx}\langle\overline{c'^2}\rangle = -U\frac{d}{dx}\left[\frac{\langle C\rangle^2}{4\pi\sigma_y\sigma_z}\right] - \frac{\alpha_c q_c}{\Lambda_c}\langle\overline{c'^2}\rangle \tag{21}$$

where α_c, q_c, and Λ_c are given by (19) using Λ_H instead of Λ.

This almost completes the specification of a practical plume model, but we generally require predictions of point values of concentration and we therefore have to make some assumption about the shape of the distribution to obtain this from the calculated integral quantities. We assume the usual Gaussian shape for the mean concentration, and the same Gaussian for the concentration variance. The latter has been shown to be correct in the meander phase of a plume in homogeneous turbulence where the variance is large, both experimentally by Fackrell and Robins (1982) and theoretically by SLP. The shape is different for surface releases and also at late times, but we shall leave improvement of the shape assumptions until further model testing warrants it.

In a boundary layer calculation, we calculate point values using reflection conditions at the surface (on both mean and variance) and also at the capping-inversion, if one exists. We calculate up to four reflected plumes (allowing for the multiple reflections of upper and lower boundaries), and limit the growth of σ_z to $0.8z_i$; where z_i is the inversion height. At this limiting value, the four reflections give a good representation of a constant value across the boundary layer.

The plume model (20), (21) has been tested against the wind-tunnel data of Fackrell and Robins. In the wind-tunnel boundary layer, the turbulence is driven by the shear at the wall, and therefore we do not have large-scale eddies producing large horizontal velocity fluctuations at the wall; hence, for these tests we set $q_s = q$, $\Lambda_H = \Lambda$. As in SLP, the observed profiles of mean velocity and turbulence correlations were used, and Λ was fixed algebraically by the equation

$$\frac{1}{\Lambda} = \frac{1}{0.65z} + \frac{1}{0.2H},$$

where H is the boundary layer thickness.

The comparisons between the predictions and observations for the plume spreads and concentration are shown for the ground release (Fig. 1) and the elevated

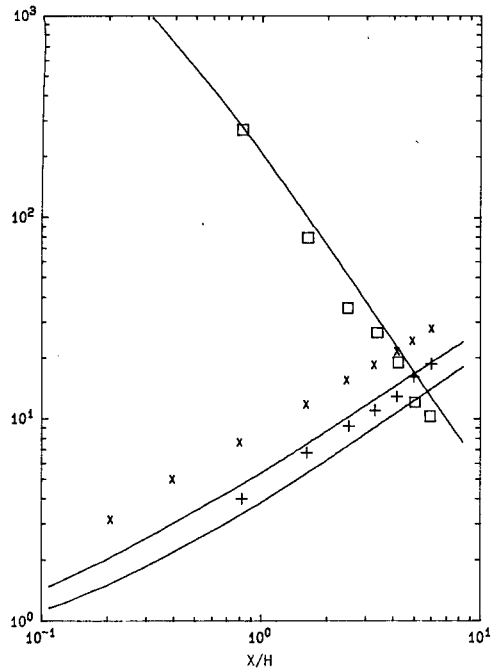

FIG. 1. Comparison of plume spread and maximum concentration (C_m) predictions with the data of Fackrell and Robins for a ground release. The symbols show the measured values: square, C_m; cross, δ_y; plus sign, δ_z.

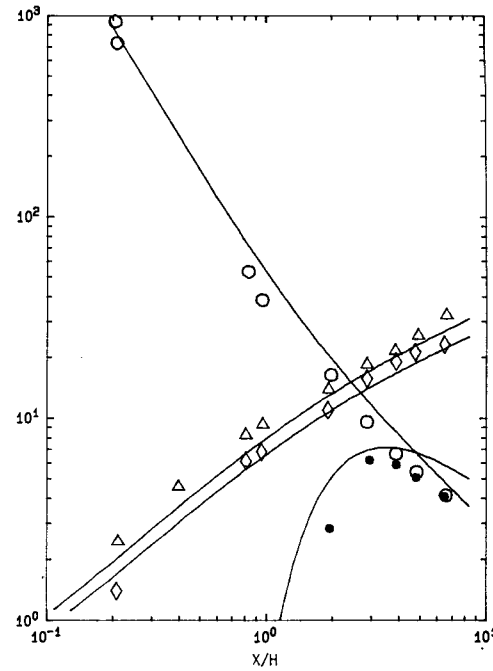

FIG. 2. As in Fig. 1, but for the elevated release; also shown is the maximum surface concentration, C_0. Symbols are as follows: open circle, C_m; solid circle, C_0; triangle, δ_y; solid diamond, δ_z.

release (Fig. 2) where δ refers to the plume width defined as the distance at which the mean concentration falls to half its maximum value. The agreement is very reasonable overall; the simplifying assumption of Gaussian distribution has not grossly misrepresented the plume. Detailed profile comparisons would not be as good as those from the full equations of SLP, but the important plume measures of Figs. 1 and 2 are predicted almost as well using the simple Gaussian model. The biggest difference appears in the underprediction of the horizontal spread of the ground release. The present integral model underpredicts this quantity by about 30%.

The model also does a very creditable job in predicting the variance magnitude, as can be seen in Fig. 3. The laboratory data show maximum rms fluctuation divided by maximum mean concentration at each x-station for different source sizes, both elevated and ground-releases. The model predictions are simply centerline values from the Gaussian, neglecting any reflection effects at the surface. We know that such effects are not negligible in these results, but the profile shapes are not well described by reflected Gaussians, and we therefore take this simple measure of fluctuation intensity to compare with the data. In the early stages of the elevated release, the profiles are very close to Gaussian, and therefore we are calculating the correct measure there. The good agreement with the elevated releases in Fig. 3 is partly to be expected, since these data were used to fix two empirical constants in the fluctuation variance equation in SLP, and this in turn forms the basis of the present model equation. The variance prediction decays more slowly than the observations; this is probably a result of our neglect of surface reflection, which decreases local intensities.

The prediction for the ground-level releases must be

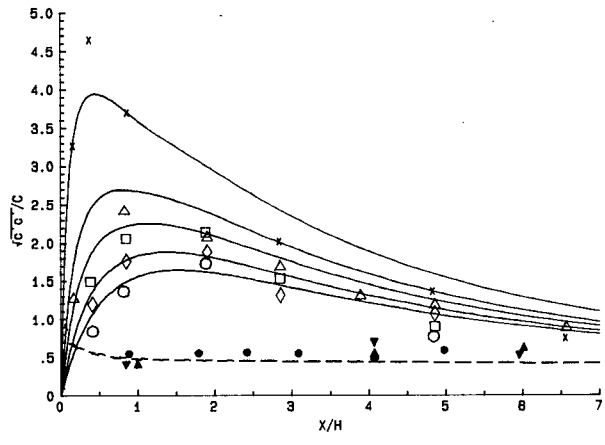

FIG. 3. Dimensionless fluctuation intensity, $\hat{c}/C_m$, for the Fackrell and Robins experiments; $\hat{c}^2$ is the maximum concentration variance. Data are for different source diameters, d_s. Elevated releases: cross, d_s = 3 mm; open triangle, 9 mm; open square, 15 mm; open diamond, 25 mm; open circle, 35 mm. Ground releases: solid triangle, 3 mm; solid dell, 9 mm; solid circle, 25 mm.

regarded as fortuitously accurate, since the fluctuation variance profiles in this case are far from Gaussian with the center on the ground. However, it should be noted that the model does correctly predict no dependence on source-size, and also that the value changes very little downstream. The ground-level fluctuation level would, in fact, be accurately predicted using the reflection conditions, but the vertical profile is poorly represented. Further data is required before rejecting the simple reflected Gaussian in favor of more complicated profiles, since the shape could depend on the type of flow, e.g., free convection versus shear-driven turbulence.

Our second comparison is with the diffusion experiments of Willis and Deardorff (1976) and Willis (1980) in a free-convection layer. The former experiment is a release near the surface at $z = 0.067h$, and the latter at $0.5h$ where h is the mixed layer depth.

The background turbulence fields were essentially taken from Willis and Deardorff (1974) observations of turbulence intensities, but some hypotheses are necessary for the length scales, and also to account for the differing horizontal and vertical scales. The vertical length scale, Λ, was taken from the Reynolds stress closure model prediction of Lewellen (1977), and Λ_H was set constant and equal to the maximum value of Λ in the domain, i.e., roughly $0.25h$. Thus, Λ_H represents the scale of the largest eddies in the flow, which we consider to extend to the surface in the horizontal fluctuations. The turbulence intensities, q and q_s, are defined as follows:

$$q^2 = \overline{u'^2} + \overline{v'^2} + \overline{w'^2} \tag{22a}$$

$$q_s^2 = (\overline{u'^2} + \overline{v'^2})\left(\frac{\Lambda}{\Lambda_H}\right)^{2/3} + \overline{w'^2} \tag{22b}$$

where $\overline{u'^2}$, $\overline{v'^2}$, $\overline{w'^2}$ are the observed turbulence intensities, q is a measure of the horizontal intensity, while q_s is a measure of the velocity scale of vertical eddies. Near the wall, the fluid motions are primarily horizontal, therefore an inertial range scaling factor is applied to obtain the energy at the scale of the vertical fluctuations. These relations are simply a means of estimating the appropriate timescales, and it is possible that theoretical analyses such as Hunt (1984) will lead

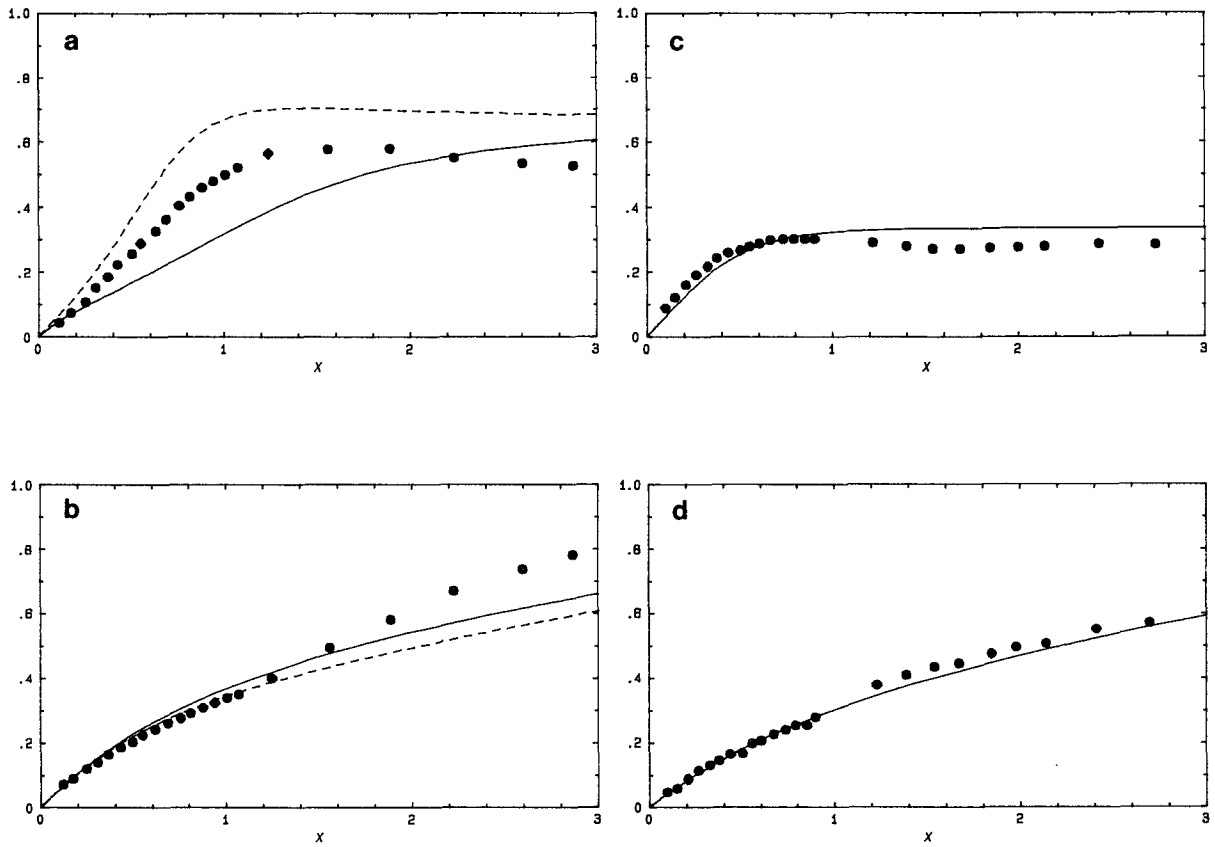

FIG. 4. Comparison of plume spread predictions with convection tank experiments; low-level release, $z_s = 0.67H$: (a) σ_z, (b) σ_y; midlevel release, $z_s = 0.5H$: (c) σ_z, (d) σ_y. Solid line shows model prediction using quasi-homogeneous equations of section 3; dashed line shows effect of including gradients of the flow variables. Data are shown as solid symbols.

to improvements. However, (22) seems to be adequate for the present state of the model.

The model predictions of σ_y and σ_z for the two releases as a function of downstream distance X from the source are compared with the observations in Fig. 4. There is reasonable agreement between the curves, with the exception of σ_z in the early part of the low release. The reason for the error can be seen in the vertical cross-sections of Willis and Deardorff (1976), where the plume is seen to lift off the ground, and behave in a very non-Gaussian fashion. Our simple model is unable to describe this complicated behavior, and this is evident in the surface concentration prediction on the plume centerline for the low release, shown in Fig. 5. There is a significant overprediction of surface impact out to about $X = 3$; the overprediction is a factor of almost 4 at the worst. As we shall demonstrate in the next section, this prediction can be dramatically improved by accounting for the inhomogeneity of the turbulent fields.

Isopleths of surface concentration for the midlevel release are shown in Fig. 6, again in comparison with observations. The main discrepancy here is an *underprediction* (by a factor of 2) of the maximum surface impact. Examination of the vertical cross-section from Willis (1980) again shows a highly non-Gaussian descent of the maximum concentration onto the surface. This feature is not in our simple model, and we consequently underpredict the impact. However, aside from the immediate vicinity of the maximum, concentrations are predicted reasonably well. Again there is an improvement by accounting for the inhomogeneity of the turbulent fields as provided by the approximations of the next section.

4. Extensions of the simple model

In this section we wish to describe some straightforward extensions of the quasi-homogeneous model of

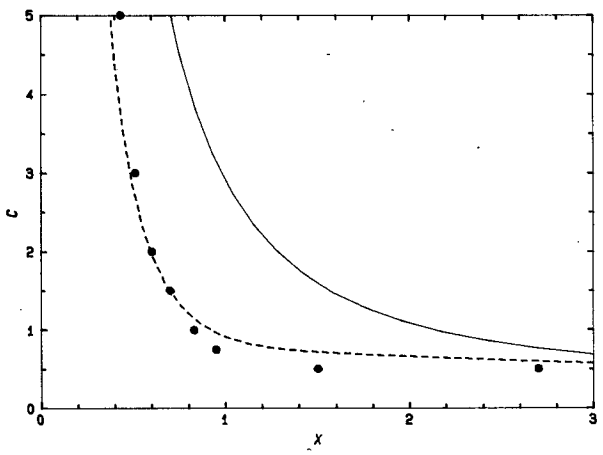

FIG. 5. Dimensionless centerline surface concentration for the low-level convective layer release. Symbols as in Fig. 4.

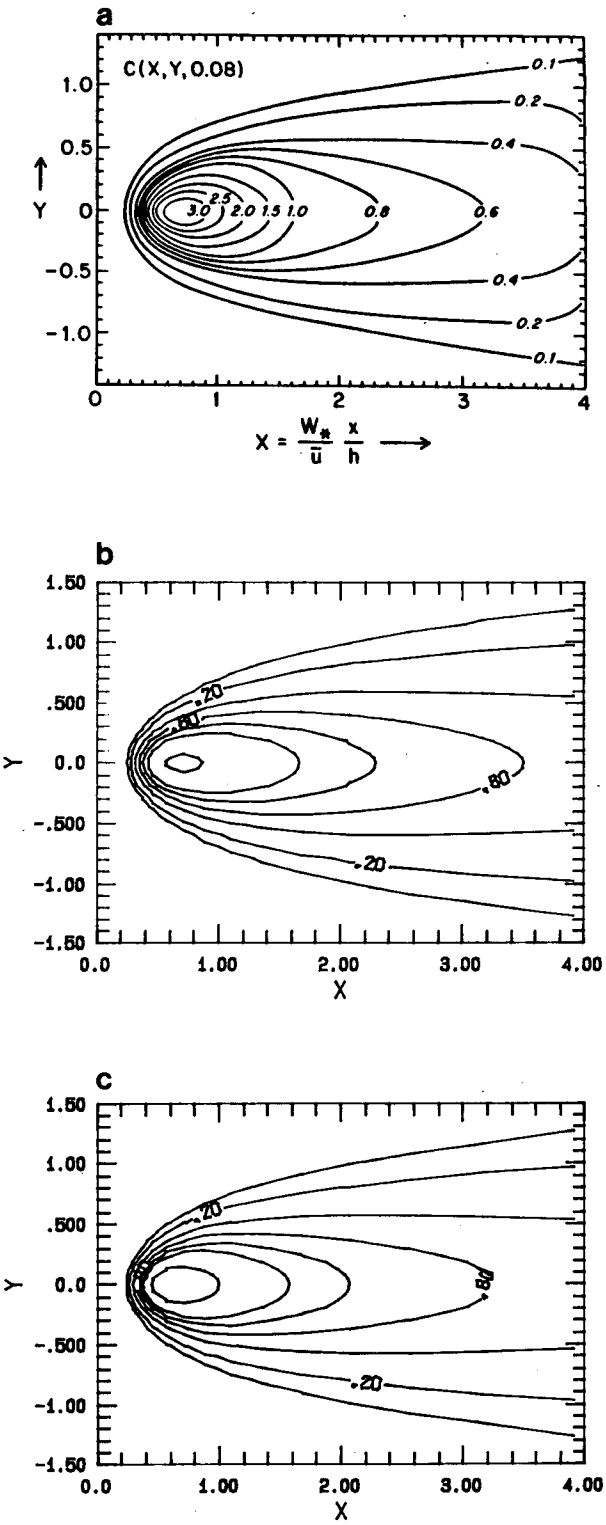

FIG. 6. Dimensionless surface concentration field for the midlevel convection layer release; (a) data of Willis (1980); (b) model prediction, and (c) model prediction including gradients of the flow variables. Vertical axis is scaled with the boundary layer depth, h; w_* is the convective scaling velocity. Isopleths are all as in (a).

the previous section to explicitly include inhomogeneity in the background flow. A bonus effect of this type of simplified modeling is that it can also provide some insight into the mechanics of such inhomogeneities. The first gradient that we consider, however, is well understood.

a. Gradients of mean velocity

In any practical prediction model, it is necessary to account for variations in wind-direction with height, because these transverse wind shears will eventually dominate the lateral dispersion of a plume. Streamwise shear is not so important since streamwise gradients are small in a plume. We therefore take as our idealized wind profile

$$\left.\begin{aligned} U &= U_0 \\ V &= \alpha(z - \bar{z}) \end{aligned}\right\},$$

where $\bar{z}$ is the plume centroid height, as usual. The transport equation for C becomes

$$U_0 \frac{\partial C}{\partial x} = -\alpha z' \frac{\partial C}{\partial y} - \frac{\partial}{\partial y}\overline{v'c'}. \tag{23}$$

The equation for $\bar{y}$ is unchanged, but that for σ_y^2 becomes

$$U_0 \frac{d}{dx}\sigma_y^2 = 2\frac{\langle y'\overline{v'c'}\rangle}{\langle C\rangle} + 2\alpha\frac{\langle y'z'C\rangle}{\langle C\rangle}. \tag{24}$$

If we write the off-diagonal moment as $\sigma_{yz}\langle C\rangle$, then the σ_y^2 equation has acquired an extra term proportional to σ_{yz}. It is easy to write a corresponding equation for σ_{yz}, and it may well be desirable to do so if one cannot specify the y- and z-axes as special coordinates. By carrying an equation for σ_{yz}, one can describe a general (i.e. tilted) Gaussian, and also account for off-diagonal Reynolds stresses. However, since our objective is a practical, atmospheric prediction model, with its necessary reflections at the ground and inversion, we suggest a simple approximation that does not require any additional equations.

We replace σ_{yz} by $\gamma\sigma_y\sigma_z$ where γ is a constant to be determined by matching with a known analytic solution. Quesada and McLeod (1971) give the solution for diffusion of a puff in a shear flow. Reducing their solution to two dimensions, the correct asymptotic match with the centerline concentration at late time is given by $\gamma = \sqrt{3}/2$. We therefore suggest this value as a simple means of incorporating wind shear effects in the model.

b. Gradients of turbulent correlations

It is a straightforward matter to consider linear variations of the background turbulent correlations with height in (8), (9). A complete analysis of all the terms is somewhat cumbersome and the complete equations are given in the Appendix, but if we leave the modeled terms (i.e., those involving Λ) in the homogeneous form, the only term that contributes to the moment equations is the production term involving $\overline{w'^2}$ in the equation for $\overline{w'c'}$. The net effect of a gradient of $\overline{w'^2}$ is to modify (11) to give

$$U\frac{d}{dx}\langle\overline{w'c'}\rangle = \frac{d\overline{w'^2}}{dz}\langle C\rangle + \frac{g}{T_0}\langle\overline{c'\theta'}\rangle - \frac{Aq}{\Lambda}\langle\overline{w'c'}\rangle. \tag{25}$$

Recalling that $\langle\overline{w'c'}\rangle$ gives the vertical motion of the plume centroid [Eq. (5)], we see that a gradient of $\overline{w'^2}$ causes a vertical motion of the plume toward regions of larger $\overline{w'^2}$. This is consistent with the observations showing plumes lifting off the ground in convectively mixed layers, which have a strong positive gradient of $\overline{w'^2}$ near the ground.

The heat flux gradient can be analyzed in a similar way; this modifies the buoyancy-correlation Eq. (14), to give

$$U\frac{d}{dx}\langle\overline{c'\theta'}\rangle = \frac{d}{dz}\overline{w'Q'}\langle C\rangle - \frac{\mathrm{dT}}{\mathrm{dz}}\langle\overline{\mathrm{w'c'}}\rangle - 2\frac{bsq}{\Lambda}\langle\overline{c'\theta'}\rangle. \tag{26}$$

We see that the effect of a negative heat flux gradient (i.e., surface heating) is to produce negative $\langle\overline{c'\theta'}\rangle$, which produces negative $\langle\overline{w'c'}\rangle$ through (25), which in turn gives a downward motion of the plume. This again is consistent with the observations, which show a descent of the plume from midlevels in the convective layer where

$$\frac{d\overline{w'^2}}{dz} = 0, \quad \frac{d\overline{w'\theta'}}{dz} < 0.$$

The details of this phenomenon are associated with the skewed distribution of vertical velocity fluctuations, and accurate simulation clearly requires account of the non-Gaussian plume profile, but the simple integrated model does appear to incorporate sufficient dynamics to model some aspects of the effect. Equation (26) shows that the unstable temperature gradient near the ground will also enhance the lift-off of a surface release. We note that the gradient terms which we have included do not involve any empirical modeling, and we therefore have some confidence that the tendencies they produce are physically realistic. The results that we now present use the full equations from the Appendix, which also include inhomogeneity in the turbulence timescale.

The effect of the gradient terms is completely negligible in the neutral boundary layer cases, but improves the prediction of the convective layer examples. For

the low-level release, Figs. 4(a) and 5 show the plume lifting off the ground and a much improved surface concentration prediction. Note that σ_z in Fig. 4(a) represents the spread of the plume about the release height, and therefore includes the rise of the plume centroid.

Figure 6 shows the surface concentration isopleths for the midlevel release. The difference here is less dramatic; in fact there is no detectable change in the plume spread, but we see that there is an increase in the initial impact on the surface that has been raised from 1.5 to 2. This is still below the observation of 3, but represents a significant improvement from the heat-flux gradient term, which causes a descent of the plume centroid. The rest of the surface impact is unaffected by the gradient terms.

5. Conclusion

A simple Gaussian plume model has been derived from the second-order closure equations for turbulent fluxes. In addition to the mean concentration, the model predicts the variance of the concentration fluctuations. This extra statistical information should prove very valuable in probabilistic assessment of the predictability of individual sampler observations. The model has the capability of utilizing spatial averages of meteorological measurements of turbulent correlations directly; on the other hand, if no turbulence data are available, some method of estimating them is required.

In comparison with laboratory experiments, the model has been shown to perform reasonably well. Convective mixed layers required the inclusion of turbulence gradients for accurate prediction. Surface concentration predictions were within a factor of 2 virtually everywhere without the need for the adjustment of empirical constants to achieve this agreement. The model is derived in a general fashion from previously determined second-order closure equations, and can, in principle, be applied to any turbulent flow. All that is necessary is a specification of the background flow and turbulence. The framework of the plume model is also seen to be flexible enough to allow incorporation of more complex effects, such as background gradients.

Acknowledgment. This work was supported by the Electric Power Research Institute under contract RP 1616-28.

APPENDIX

Equations for Inhomogeneous Turbulence

In order to account for gradients in the background fields, we assume a linear local variation in the vertical direction, i.e.,

$$\overline{w'^2} = \overline{w_0'^2} + z' \frac{d}{dz}\overline{w'^2}$$

$$\Lambda = \Lambda_z + z' \frac{d\Lambda_z}{dz}$$

$$q^2 = q_s^2 + z' \frac{d}{dz} q_s^2, \quad \text{etc.}$$

These forms are substituted into the second-order closure equations prior to integrating over the plume, and we expand the gradient terms and retain only the first term linear in z, i.e., we assume the gradients are small in the sense that the variation over the plume width is small. This results in the following integral equations.

$$\left.\begin{aligned}
U_0 \frac{d}{dx}\langle y'\overline{v'c'}\rangle &= \overline{v_0'^2}\langle C\rangle - \frac{\langle y'\overline{v'c'}\rangle}{\tau_{vc}} + 2\gamma\sigma_y\sigma_z\frac{dV}{dz} \\
U_0 \frac{d}{dx}\langle z'\overline{w'c'}\rangle &= \overline{w_0'^2}\langle C\rangle + \frac{g}{T_0}\langle z'\overline{c'\theta'}\rangle - A/\tau_1 \frac{\langle z'\overline{w'c'}\rangle}{\tau} \\
U_0 \frac{d}{dx}\langle z'\overline{c'\theta'}\rangle &= -\frac{dT}{dz}\langle z'\overline{w'c'}\rangle + \overline{w'\theta'_0}\langle C\rangle - 2bs/\tau_1 \frac{\langle z'\overline{c'\theta'}\rangle}{\tau} \\
U_0 \frac{d}{dx}\langle \overline{w'c'}\rangle &= \frac{g}{T_0}\langle \overline{c'\theta'}\rangle + \frac{d}{dz}\overline{w'^2}\langle C\rangle - A/\tau_2 \frac{\langle \overline{w'c'}\rangle}{\tau} - A\frac{\langle z'\overline{w'c'}\rangle}{z_1\tau_z} \\
U_0 \frac{d}{dx}\langle \overline{c'\theta'}\rangle &= -\frac{dT}{dz}\langle \overline{w'c'}\rangle + \frac{d}{dz}\overline{w'\theta'}\langle C\rangle - 2bs\frac{\langle \overline{c'\theta'}\rangle}{\tau_2} - 2bs\frac{\langle z'\overline{c'\theta'}\rangle}{z_1\tau_z}
\end{aligned}\right\},$$

where

$$\left.\begin{aligned}
\frac{1}{\tau_{vc}} &= \frac{Aq}{\Lambda_H} \\
\frac{1}{\tau_1} &= \frac{q_s}{\Lambda_z}\left[1 - \frac{3\sigma_z^2}{2q_s^2\Lambda_s}\frac{dq_s^2}{dz}\frac{d\Lambda_z}{dz}\right] \\
\frac{1}{\tau_2} &= \frac{q_s}{\Lambda_z}\left[1 - \frac{\sigma_z^2}{q_s^2\Lambda_s}\frac{dq_s^2}{dz}\frac{d\Lambda_z}{dz}\right] \\
\frac{1}{\tau_z} &= \frac{q_s}{\Lambda_z} \\
\frac{1}{z_1} &= \frac{1}{2q_s^2}\frac{dq_s^2}{dz} - \frac{1}{\Lambda_z}\frac{d\Lambda_z}{dz}
\end{aligned}\right\}.$$

All background values refer to an average over the plume using the triangular filter as described in section

3, with the exception of the temperature gradient, which is also weighted by the height, z, in order to remove the singularity at the surface.

REFERENCES

Fackrell, J. E., and A. G. Robins, 1982: Concentration fluctuations and fluxes in plumes from point sources on a turbulent boundary layer. *J. Fluid Mech.*, **117,** 1–26.

Hunt, J. C. R., 1984: Turbulence structure in thermal convection and shear-free boundary layers. *J. Fluid Mech.*, **138,** 161–184.

Kaimal, J. C., 1978: Horizontal velocity spectra in an unstable surface layer. *J. Atmos. Sci.*, **35,** 18–24.

Lewellen, W. S., 1977: Use of invariant modeling. *Handbook of Turbulence,* W. Frost and T. M. Moulder, Eds., Plenum, 237–280 pp.

——, 1981: Modeling the lowest 1 km of the atmosphere. AGARD-AG-267.

——, and R. I. Sykes, 1983: On the use of concentration variance predictions as a measure of natural uncertainty in observed concentration samples. *Proc., Sixth Symp. on Turbulence and Diffusion,* Boston, Amer. Meteor. Soc., 47–50.

Pasquill, F., and F. B. Smith, 1983: *Atmospheric Diffusion,* Ellis Horwood.

Quesada, A. F., and M. A. McLeod, 1971: The determination of diffusion coefficients in a shearing flow by chemical tracer techniques. *Symp. Air Pollution Turbulence Diffusion,* Amer. Meteor. Soc., 384–391.

Sykes, R. I., W. S. Lewellen and S. F. Parker, 1984: A Turbulent-transport model for concentration fluctuations and fluxes. *J. Fluid Mech.*, **139,** 193–218.

Taylor, G. I., 1921: Diffusion by continuous movements. *Proc. London Math. Soc. (Ser. 2),* **20,** 196–211.

Willis, G. E., 1980: Laboratory modeling of dispersion in the convectively mixed layer. *Fifth Symp. on Turbulence Diffusion and Air Pollution,* Amer. Meteor. Soc., 155–156.

——, and J. W. Deardorff, 1974: A laboratory model of the unstable planetary boundary layer. *J. Atmos. Sci.*, **31,** 1297–1307.

——, and ——, 1976: A laboratory model of diffusion into the convective planetary boundary layer. *Quart. J. Roy. Meteor. Soc.*, **102,** 427–445.